

Ultrasonic Assisted Synthesis and Characterization of $x\text{CuO}/\text{CeO}_2-\gamma\text{Al}_2\text{O}_3$ Nanocatalysts

A. Karimi, E. Fatehifar*, R. Alizadeh, M. Jamili, A. Jafarizad

Environmental Engineering Research Center (EERC), Faculty of Chemical Engineering, Sahand University of Technology, Sahand New Town, Tabriz, Iran

ARTICLE INFO

Article history:

Received: 2015-09-19

Accepted: 2016-04-18

Keywords:

Selective Oxidation

CuO/CeO_2

Alumina

Ultrasound Energy

nanocrystal

ABSTRACT

In this paper, $x\text{CuO}/\text{CeO}_2-\gamma\text{Al}_2\text{O}_3$ nano-catalysts were successfully synthesized by precipitation method and modified via ultrasonic waves. For characterization of $x\text{CuO}/\text{CeO}_2-\gamma\text{Al}_2\text{O}_3$ samples N_2 adsorption results showed that the BET surface area of the $\text{CuO}/\text{CeO}_2-\gamma\text{Al}_2\text{O}_3$, X-ray diffraction (XRD), scanning electron microscope (SEM) and energy dispersive X-rays (EDX dot-mapping) were used. The BET, XRD and SEM results indicate that $\text{CuO}/\text{CeO}_2-\gamma\text{Al}_2\text{O}_3$ particles are nano-structured catalysts. These catalysts ($x\text{CuO}/\text{CeO}_2-\gamma\text{Al}_2\text{O}_3$) have high specific surface and finer particle that confirm SEM pictures. $x\text{CuO}/\text{CeO}_2-\gamma\text{Al}_2\text{O}_3$ catalyst compared to other previous synthesis catalysts for selective CO oxidation. The activity and selectivity of these catalysts obtained in the presence of rich hydrogen stream, with space velocity of $30,000 \text{ h}^{-1}$ in the absence of CO_2 and H_2O . Results show that $\text{CuO}/\text{CeO}_2-\gamma\text{Al}_2\text{O}_3$ demonstrate high CO conversion in temperature less than 120°C , and selectivity of more than 63% at 100°C . Also, results show that decreasing of CeO_2 amount decreases selectivity of CO oxidation.

1. Introduction

Today, one method of hydrogen production is via steam methane-reforming in refineries, which is used for hydrocracking, hydrodesulphurization. The reformate gases that are produced in this reaction contain about 0.5–1% carbon monoxide, 50% H_2 , 20% CO_2 , 10% H_2O and N_2 [1]. Reforming must be followed by gas conditioning, gas separation and purification stages because the catalysts used in the refinery and petrochemical plants will be contaminated by carbon monoxide at

lower than 100 ppm, and fuel cells are highly sensitive to even trace amounts of carbon monoxide [2]. Therefore carbon monoxide must be made less to below these levels to prevent these hardships. Among other processes, the methanation and catalytic selective carbon monoxide oxidation are the choices to reduce the carbon monoxide content in the reformed gas to satisfactory levels. Catalytic selective oxidation of carbon monoxide seems to be a straightforward and cost effective method to achieve acceptable

*Corresponding author: fatehifar@sut.ac.ir

carbon monoxide concentrations [3]. For an efficient PROX¹ reaction, the catalyst used in the reaction should demonstrate high catalytic activity and high selectivity for the carbon monoxide oxidation in order to minimize consumption of the H₂. Various catalytic systems have been proposed in the literature for the selective oxidation of carbon monoxide in H₂ rich streams. As an example, platinum group metals (Pt, Pd, Ru and Rh) catalysts, gold-based catalysts and transition metal-based catalysts (Cu, Co and Mn) were used for selective CO oxidation [4-12]. The CuO/CeO₂ represents one of the most interesting catalysts, which results in more active, selective and convenient thermally stable catalysts than Pt or Au based ones [13–15]. The absence of precious metals in the composition of these catalysts is a remarkable economic advantage. In this research, $x\text{CuO}/\text{CeO}_2-\gamma\text{Al}_2\text{O}_3$ catalysts were prepared by the precipitation method and their catalytic performance was tested for PROX of CO in H₂-rich gas streams. Finally, these catalysts were compared with our previous catalysts in CO oxidation. This synthesis method has been chosen for the following reasons. The powerful waves of ultrasound, due to turbulent flow and shock waves, metal particles can move toward each other with high-speed and also may melt at collision point [16]. The suspension solution occurs because of Inter-particle collisions which occur very quickly, as a result, the mass of the particle is formed. Collisions can cause a crushing blow between particles, and so increased specific surface, and finally to achieve high reactivity and good conversion. The impregnation-ultrasound method in comparison with other methods such as sol-gel [17], co-precipitation and

impregnation [14] and citrate method [18] has high specific surface, high conversion, selectivity and finer particles that confirm in SEM pictures.

2. Experimental works

2.1. Catalyst preparation

The precipitation method was used for preparation of CuO/CeO₂- γ Al₂O₃ nanocatalysts. Cu (NO₃)₂·3H₂O, Ce (NO₃)₃·6H₂O, Urea and Al (NO₃)₃·9H₂O (all of them from Merck) were used as metal precursors. In this work, five types of catalysts ($x\text{CuO}/\text{CeO}_2-\gamma\text{Al}_2\text{O}_3$) were synthesized, x is 5, 7, 10, 12.5, and 15%. Required amounts of the metal salts for catalyst preparation were dissolved in 100 mL de-ionized water. To improve metal distribution in catalysts, Bandelin 3200 ultrasound apparatus with 70 w was used. For control of solution temperature and keeping it at 35°C during the process, ice-water bath was used. The solution took over 40 minutes under the influence of ultrasound waves. The catalysts were subsequently dried at 110°C for 48 h and finally calcined for 5 h at 500°C under continuous air flow at a given heating rate (hr=10°C/min). The algorithm of synthesis is shown in Fig. 1.

2.2. Catalyst characterization

The specific surface areas of the catalysts were determined by means of nitrogen physisorption, at -196°C using Quanta chrome ChemBET3000 instrument. The XRD was used to identify the phases present and carried out by D5000 Siemens device 30kV and 20mA with scan rate of 0.04 1/s. The average crystallite sizes were calculated from the peak width using Scherer's equation [19].

$$D = 0.9\lambda / (\beta \cos\theta) \quad (1)$$

¹ Preferential Oxidation

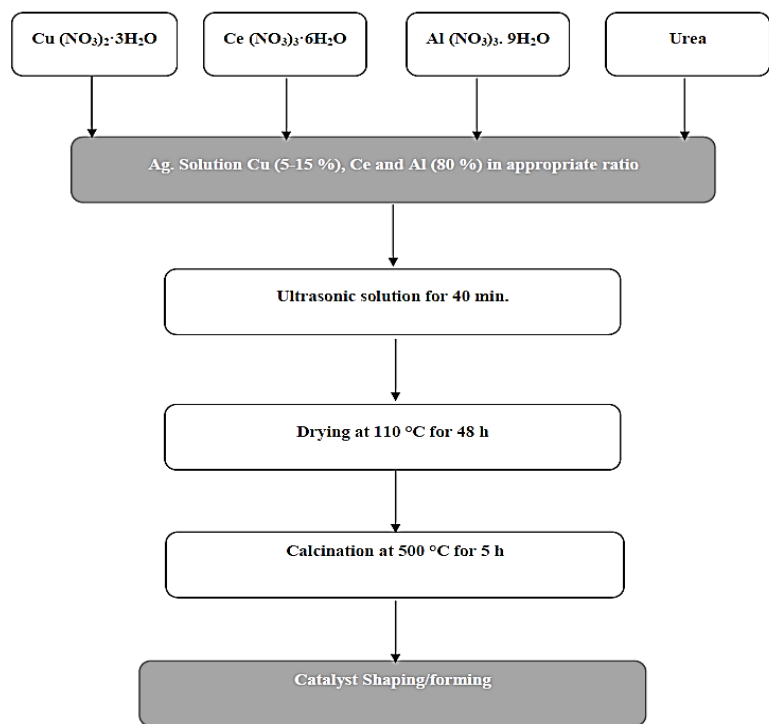


Figure 1. The schematic diagram of catalyst algorithm synthesis $x\text{CuO}/\text{CeO}_2-\gamma\text{Al}_2\text{O}_3$ catalysts.

SEM analysis was performed on JEM100CX scanning electron microscope and the samples were first sputtered with Au for observing morphology and particle size of nanostructure catalysts. Energy dispersive X-ray analysis (EDX) was carried out by SAMx with DXP-X10P processor for elemental analysis.

2.3. Catalyst activity test

The catalytic oxidation of CO was carried out in a fixed-bed reactor system at atmospheric pressure (with the difference being that reactor is placed out of furnace, in most of the pilots fixed-bed reactor is placed in the furnace). After heating gas in the furnace, it passes from the reactor. The reactor was a 4 mm I.D. (6-mm O.D.). Prior to all catalytic tests, the samples were heated in a flowing 20 vol.% O_2/N_2 mixture at 300 °C for 40 min as a standard pretreatment, followed by cooling down to the reaction temperature in pure N_2 . The catalyst weight was 200-300 mg and the total flow rate of the reaction mixture

consisted of 1 vol.% CO, 1 vol.% O_2 and 50 vol.% H_2 in N_2 balance was adjusted to 200-400 $\text{mL}\cdot\text{min}$. The gas lines were heated in order to avoid water condensation before the reactor inlet. The reactor effluent was passed through an ice-cooled water condenser to remove water vapor before inlet GC for analysis. The main oxidation reactions are as follow [16]:

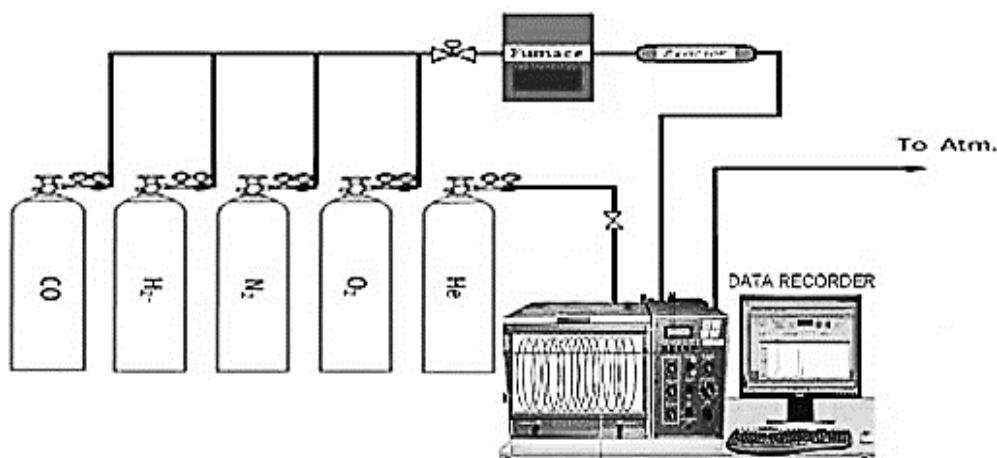
Desired reaction



Undesired reaction



Reactant and product components were analyzed online by a gas chromatograph (Agilent Technologies 7890A Network GC system) equipped with a thermal conductivity detector (TCD) that was used to analyze the outlet composition. HP-Plot Q column (Agilent) was used; with helium as carrier. The CO conversion was based on the carbon monoxide consumption in the reaction as follows:

**Figure 2.** Schematic diagram of the experimental setup.

$$\text{Activity}(\%) = \frac{[\text{CO}_2]_{\text{out}}}{[\text{CO}_2]_{\text{out}} + [\text{CO}]_{\text{out}}} \times 100 \quad (4)$$

The selectivity is defined as the oxygen consumed by CO oxidation, namely:

$$\text{Selectivity} (\%) = \frac{0.5[\text{CO}_{\text{in}} - \text{CO}_{\text{out}}]}{[\text{O}_2]_{\text{in}} - [\text{O}_2]_{\text{out}}} \times 100 \quad (5)$$

3. Results and discussion

Catalysts were characterized by using different techniques. BET surface area and particle sizes of catalysts are shown in Table 1. BET surface areas of the $\text{CuO}/\text{CeO}_2-\gamma\text{Al}_2\text{O}_3$ catalysts have greater surface in comparison with CuO/CeO_2 catalyst [16,19]. The evaluation of samples show with increase of loading Cu decreased specific surface areas of the catalysts. The reason cans be active phase on surface of the support; with a simple geometrical approximation of the BET analysis it was shown that synthetic catalysts are nanometer in size [20].

The X-ray diffraction results of the $\text{CuO}/\text{CeO}_2-\gamma\text{Al}_2\text{O}_3$ catalysts after calcination are shown in Fig. 3. The XRD patterns of the samples showed no CuO reflections in less than 12.5% loading of Copper, indicating that the copper oxide phase exists in a highly divided or amorphous state in these catalysts or better dispersion of CuO on the surface of

Table 1.
Surface area and particle sizes of $\text{CuO}/\text{CeO}_2-\gamma\text{Al}_2\text{O}_3$ prepared catalysts.

Catalyst	S (m^2/g)	Particle size (nm)
%5 $\text{CuO}/\text{CeO}_2-\gamma\text{Al}_2\text{O}_3$	167	24
%7 $\text{CuO}/\text{CeO}_2-\gamma\text{Al}_2\text{O}_3$	159	26
%10 $\text{CuO}/\text{CeO}_2-\gamma\text{Al}_2\text{O}_3$	148	29
%12.5 $\text{CuO}/\text{CeO}_2-\gamma\text{Al}_2\text{O}_3$	140	33
%15 $\text{CuO}/\text{CeO}_2-\gamma\text{Al}_2\text{O}_3$	132	35

ceria and alumina [21]. Table 2 indicated crystal size of catalysts from Scherer's equation.

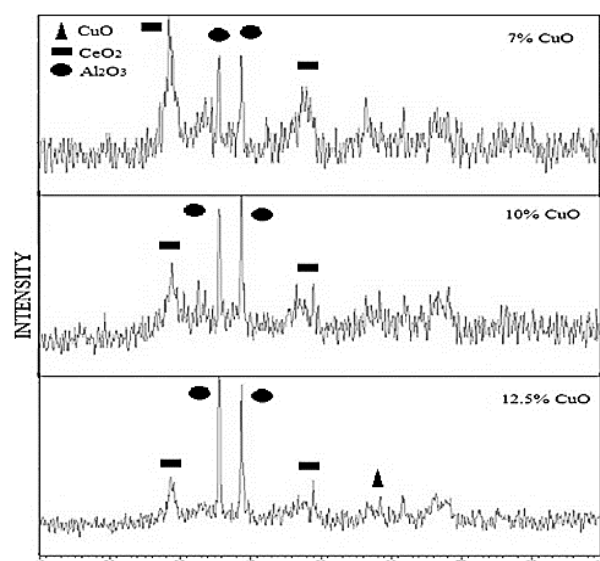
**Figure 3.** XRD spectra of $\text{CuO}/\text{CeO}_2-\gamma\text{Al}_2\text{O}_3$ catalysts prepared.

Table 2.

The crystal size of prepared catalysts from Scherer's equation.

Catalyst	Max. peak angle (2θ)	Crystal size (nm)
%10 CuO/CeO ₂ -%80 γ Al ₂ O ₃	38.98	27
%12.5 CuO/CeO ₂ -%80 γ Al ₂ O ₃	35.83	34

Fig. 4 demonstrates the SEM images of the fresh CuO/CeO₂- γ Al₂O₃ catalysts. It is apparent that CuO/CeO₂- γ Al₂O₃ have different particle size with CuO loading varying from 5 to 10% CuO.

Figs. 5 & 6 show EDX dot-mapping analyses for CuO/CeO₂ nanocatalysts, and Figs. 7 & 8 show analyses for CuO/CeO₂- γ Al₂O₃ nanocatalysts. From EDX dot-mapping analysis of CuO/CeO₂, well dispersion of Cu particles can be concluded. Cu and Ce in CuO/CeO₂- γ Al₂O₃ nanocatalyst also have good dispersion. This observation

confirms the effect of ultrasonic in improving the dispersion of active phase over support. EDX dot-mapping pictures show dispersion in micro scale and in this scale all particles (Cu, Ce and Al) are well dispersed. Comparing EDX dot-mapping analysis of CuO/CeO₂ and CuO/CeO₂- γ Al₂O₃ nanocatalysts, dispersion of 7% Cu is better than dispersion of 10% Cu.

The activity and selectivity obtained with the CuO/CeO₂- γ Al₂O₃ catalysts for the selective oxidation of CO in the presence of excess hydrogen were presented in Fig. 9, 10 and Fig. 11. Figs. 9 and 10 show the effect of Cu loading of the catalysts on CO conversion in CO oxidation in the absence of CO₂ and H₂O (1% CO, 1% O₂, 50 H₂ and balance N₂). Fig. 9 presents the CO conversion of four impregnation-ultrasound prepared catalysts,

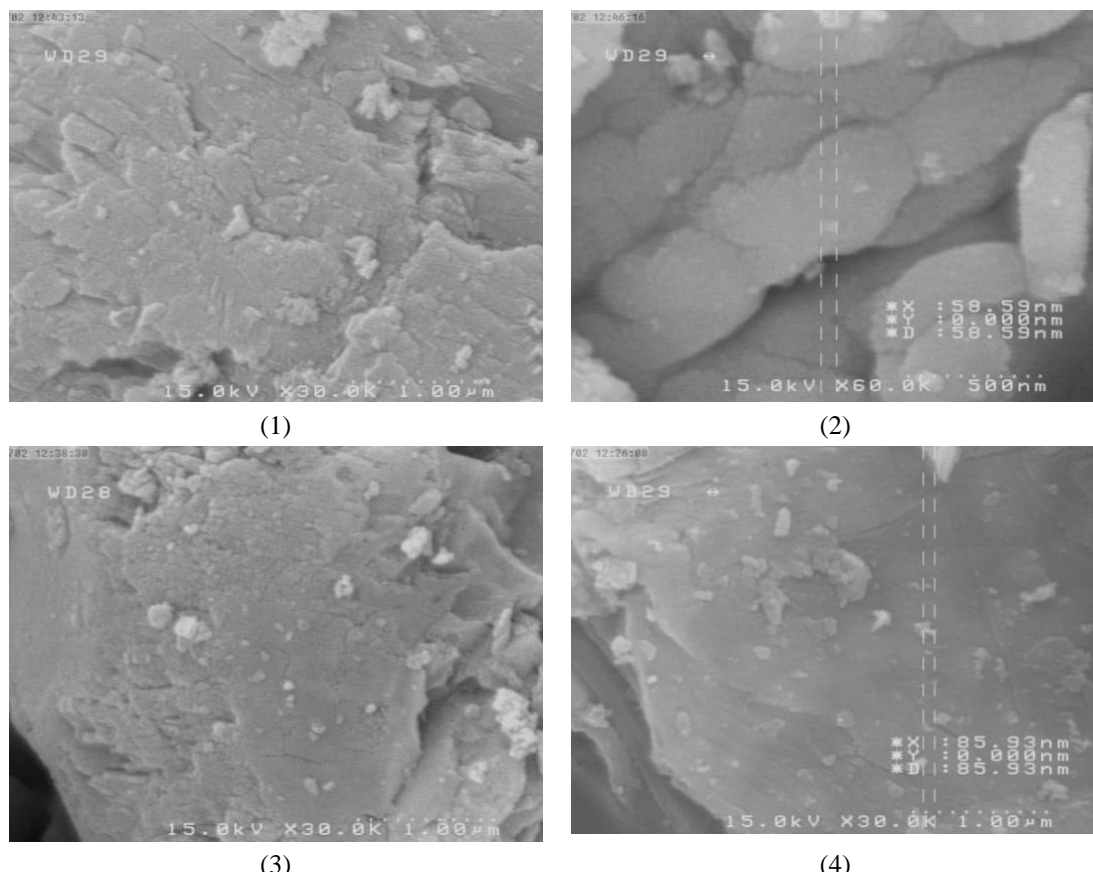


Figure 4. SEM photographs of fresh CuO/CeO₂- γ Al₂O₃ catalysts(1,2) 10% CuO scale bar 1.00 μ m (3) 7% CuO scale bar 3.00 μ m (4) 5% CuO scale bar 1.00 μ m.

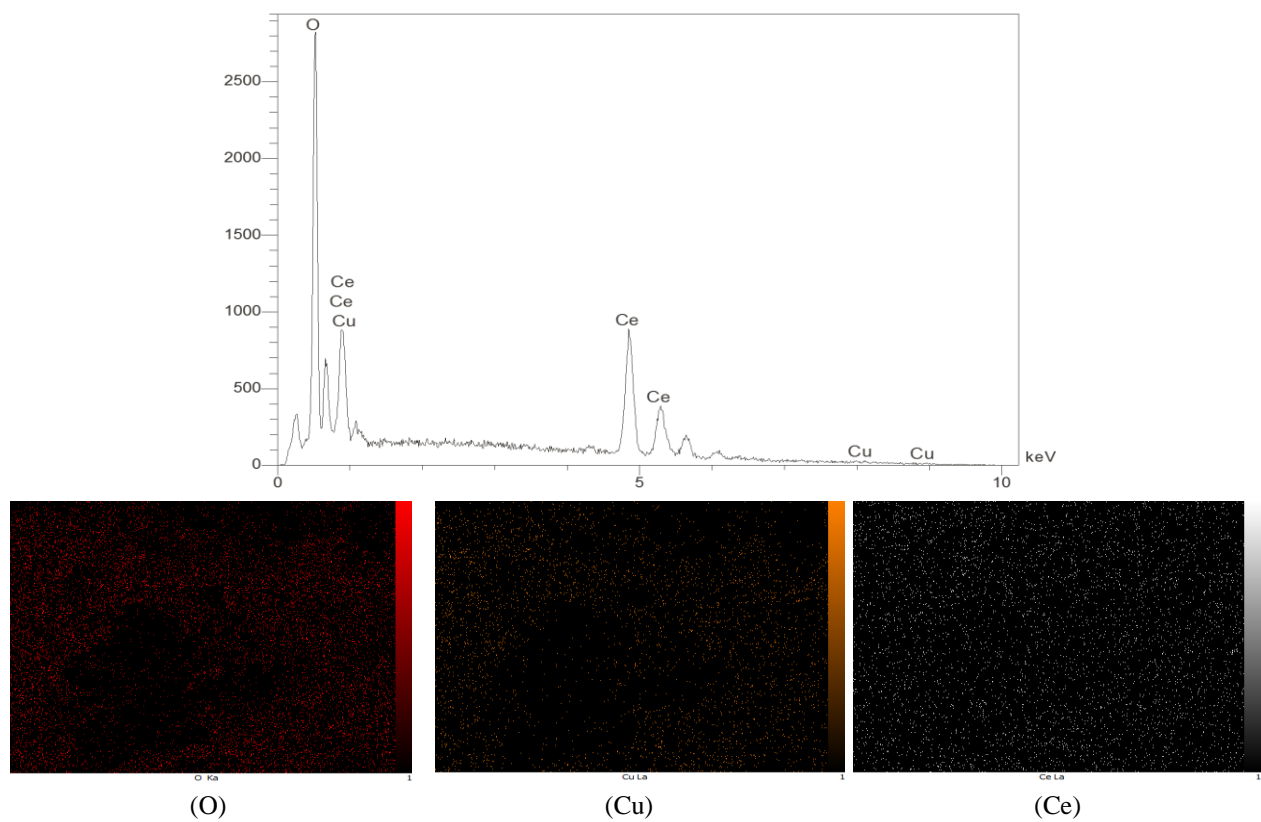


Figure 5. EDX dot-mapping analysis 10% CuO/CeO₂

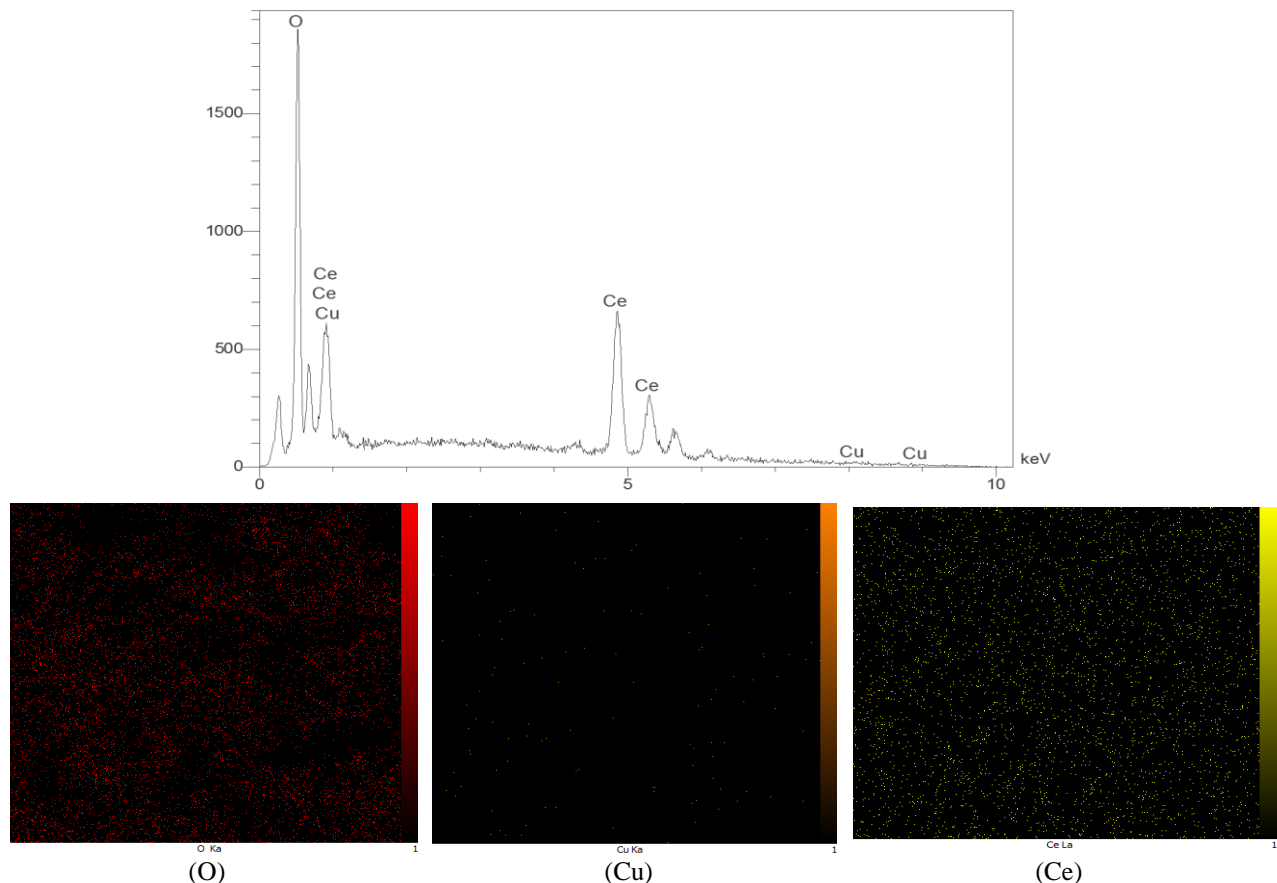


Figure 6. EDX dot-mapping analysis 7% CuO/CeO₂.

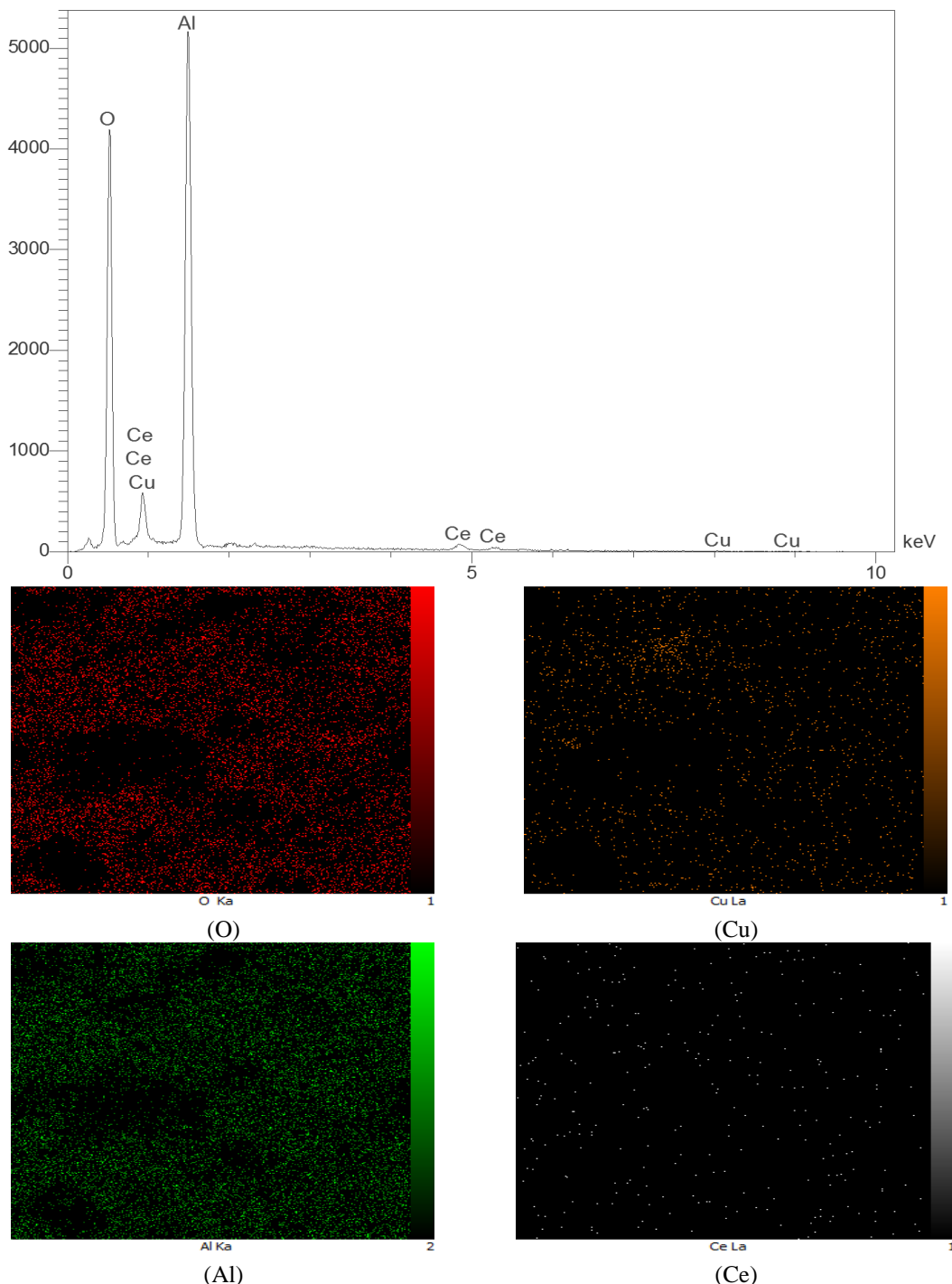


Figure 7. EDX dot-mapping analysis 10% CuO/CeO₂- γ Al₂O₃.

namely 5% Cu, 7% Cu, 10% Cu and 12.5% Cu. The 7% Cu, 10% Cu catalysts appeared to be the most active. Comparable results were previously reported in the literature by Avgouropoulos *et al.* [22] who observed that, among their three CuO/CeO₂ prepared catalysts by co-precipitation, the 14.3% Cu

catalyst was more active than the 7.3 or 20.9% Cu catalysts in CO oxidation. Using a 30000 1/h gas hourly space velocity (GHSV), 100% CO conversion can be achieved at 100°C. As can be seen, the reactor is located outside of furnace. The reaction temperature is lower than the previous works [14,17,18].

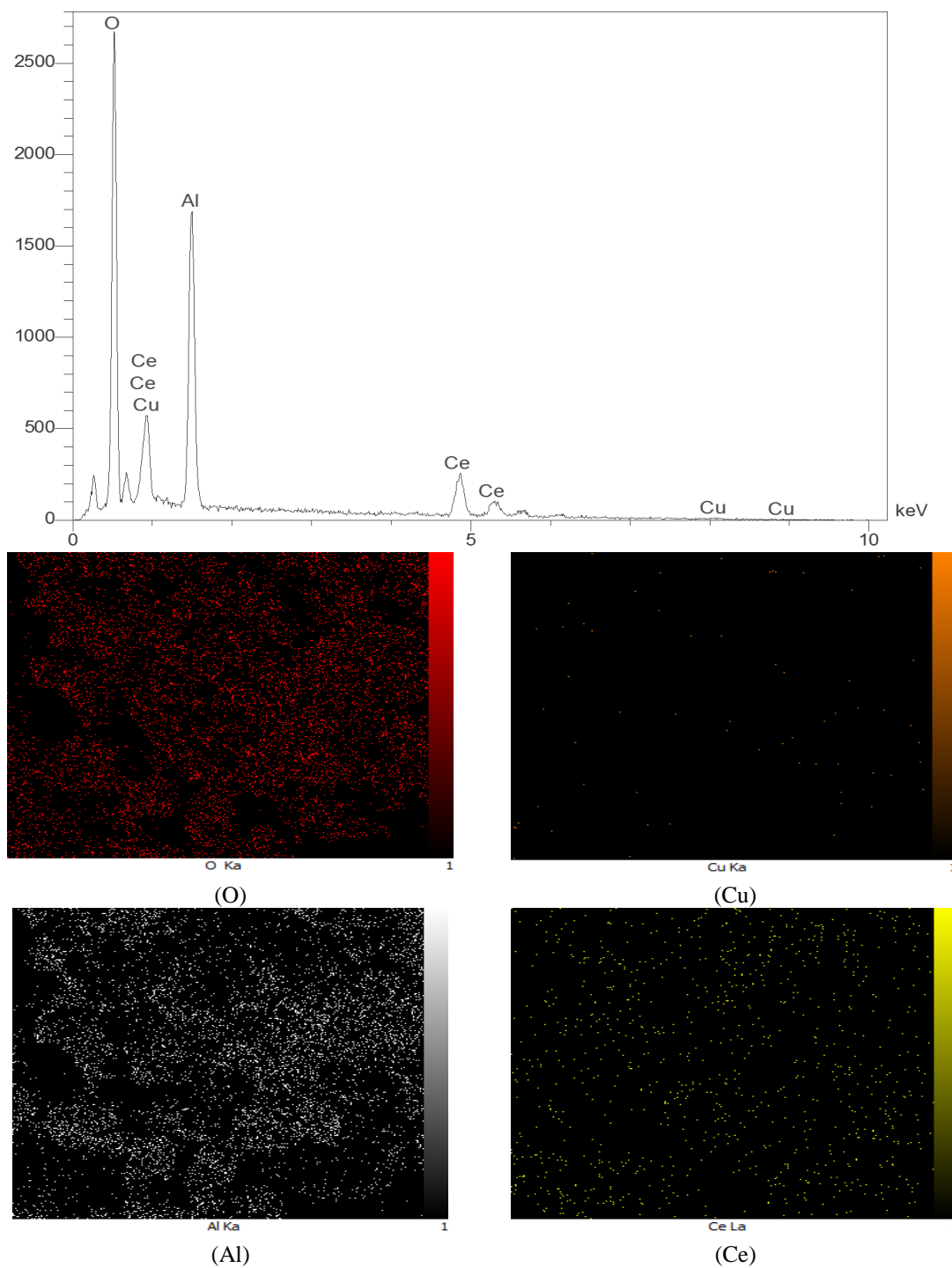


Figure 8. EDX dot-mapping analysis 7% CuO/CeO₂-γAl₂O₃.

Fig. 10 presents the CO conversion of four impregnation-ultrasound CuO/CeO₂-γAl₂O₃ catalysts. By comparing CuO/CeO₂ catalyst it was observed that CuO/CeO₂-γAl₂O₃ catalysts have weak conversion, so CuO/CeO₂ catalyst established the effective interaction between the base catalyst (CeO₂) and active metal,

indeed ceria has the ability to absorb oxygen and create CO, which makes better oxidation with high activity. Fig. 11 presents the CO selectivity of two impregnation-ultrasound prepared samples, namely 7% Cut and 10% CuO/CeO₂. Using a 30000 1/h GHSV, 100% CO conversion was attained with 86%

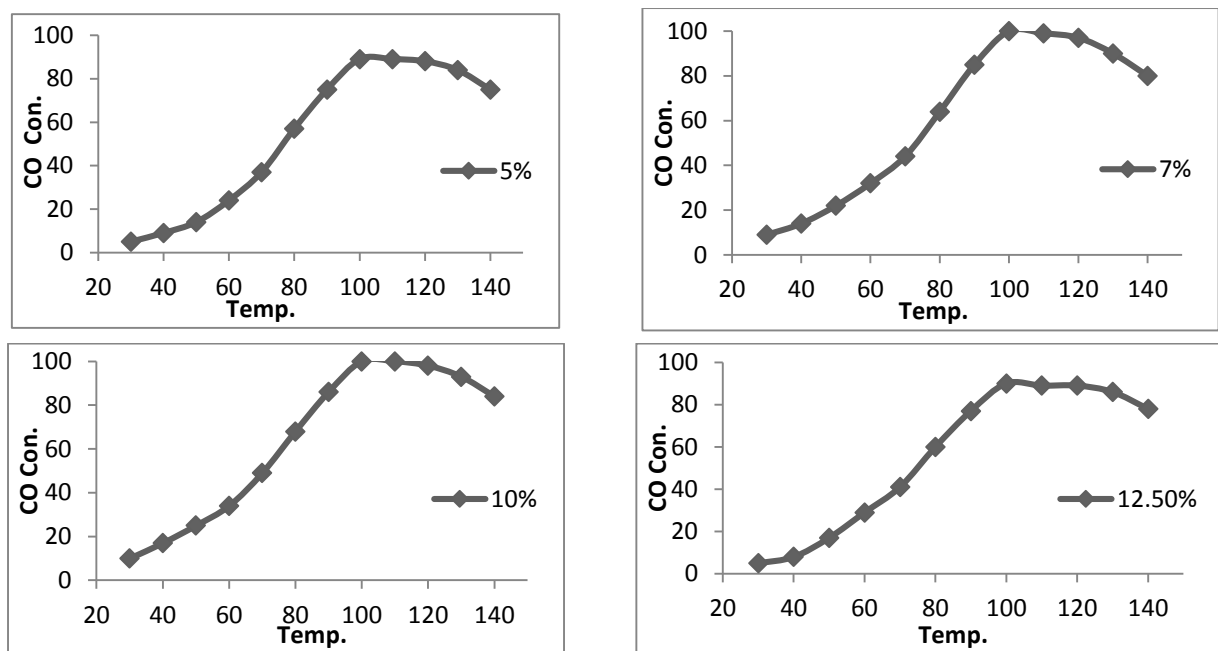


Figure 9. Variation of CO conversion CuO/CeO₂ catalyst [16].

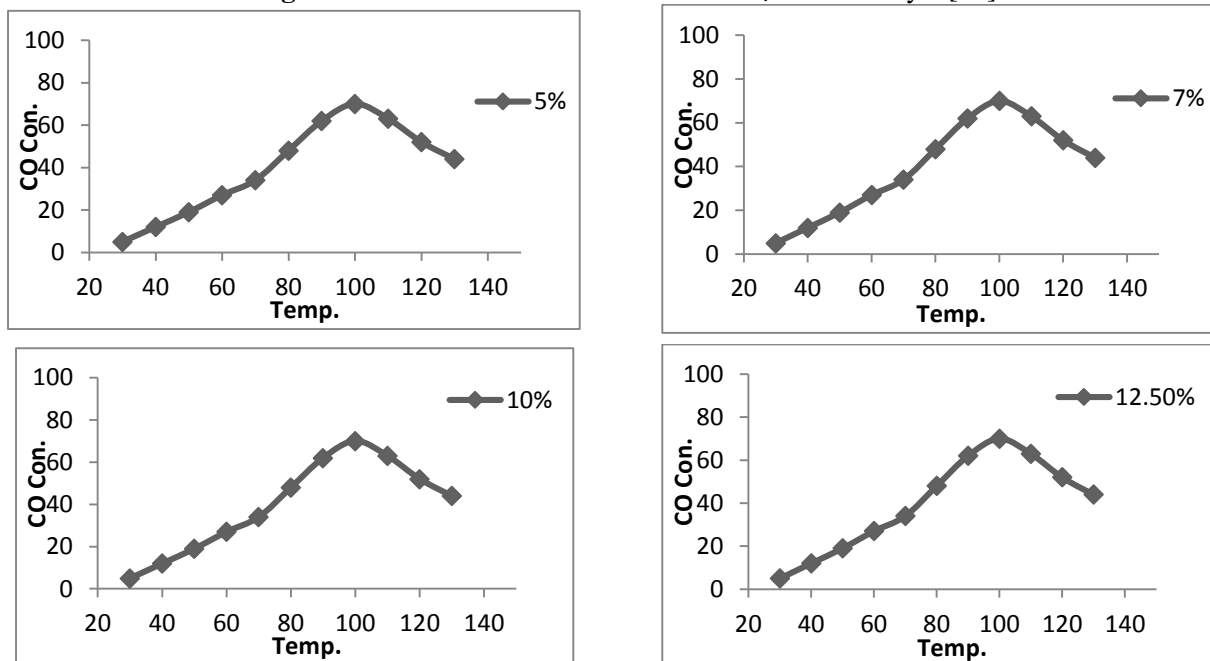


Figure 10. Variation of CO conversion CuO/CeO₂- γ Al₂O₃ catalyst.

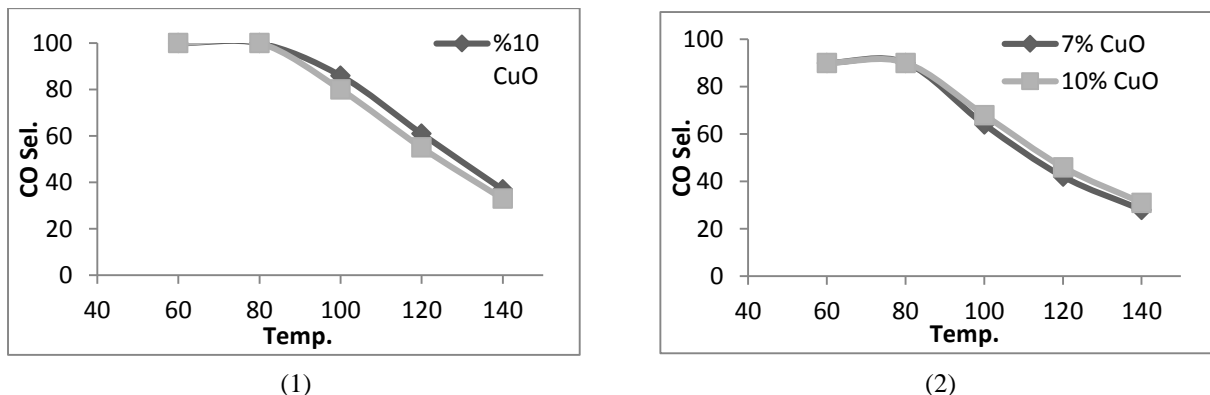


Figure 11. Variation of CO selectivity (1) CuO/CeO₂ [16] (2) CuO/CeO₂- γ Al₂O₃ catalyst.

selectivity for CuO/CeO₂ samples [16], and 70% CO conversion with 63% selectivity for CuO/CeO₂- γ Al₂O₃ at 100°C, but these samples have good conversion and selectivity in comparison with CuO/CeO₂- γ Al₂O₃ catalyst that has been prepared other synthesis method [19]. This catalyst (with this method) exhibits very high activity and selectivity for PROX of CO in H₂. Regardless of the presence of 50 vol. % H₂ in the feed, no H₂ at all was oxidized at temperatures lower than 60-80°C, indicating that the catalyst was almost inactive for the oxidation of H₂ in the low temperature regime. Nevertheless, the selectivity decreased gradually with the increase of reaction temperature.

4. Conclusions

CuO/CeO₂- γ Al₂O₃ catalysts with Cu loading in the range 5–15 wt%, and 80 wt% γ Al₂O₃, were prepared by impregnation-ultrasound method and studied in both the CO oxidation and the selective CO oxidation in excess hydrogen. The following main conclusions may be drawn from this research:

The BET, XRD and SEM results indicate that CuO/CeO₂- γ Al₂O₃ particles are nanostructured catalysts. BET showed that these catalysts have high specific surface in comparison with other methods. XRD invisible CuO species were synthesized with ultrasound method of the CuO phase on the alumina confirmed in high percentages. SEM analysis indicated CuO/CeO₂- γ Al₂O₃ catalysts containing highly dispersed. EDX dot-mapping suggests that ultrasonic waves cause well dispersion of Cu, Ce and Al particles. The pilot was designed such that reactor would be out of the furnace. The impregnation-ultrasonic CuO/CeO₂- γ Al₂O₃ catalysts are very active and remarkably selective for the CO oxidation in the presence of excess

hydrogen in comparison with other methods such as citrate and impregnation. CO conversion higher than 70% with selectivity of 63% can be obtained for this catalyst at 90–110 °C and a space velocity of 30,000 1/h in the absence of CO₂ and H₂O.

References

- [1] Marschner, F. and Moeller, F. W., "Methanol Synthesis", Applied Industrial Catalysis, Academic Press in: B.E. Leach (Ed.). 215 (1983).
- [2] Tanaka, H. Kuriyama, M. Ishida. Y. Ito, S. I. Tomishige, K. and K. Kunimori, "Preferential CO oxidation in hydrogen-rich stream over Pt catalysts modified with alkali metals", *Appl. Catal. A.*, **343** (1-2), 117 (2008).
- [3] Shen, W. J. Ichihashi, Y. Ando, H. Matsumura, Y. and Haruta, m., "Effect of reduction temperature on structural properties and CO/CO₂ hydrogenation characteristics of a Pd–CeO₂ catalyst", *Appl. Catal. A.*, **217** (1-2), 231 (2001).
- [4] Pozdnyakova, O. D. Teschner, A. Wootsch, J. Krohnert, B. Steinhauer and H. Sauer, "Preferential CO oxidation in hydrogen (PROX) on ceria-supported catalysts, part II: oxidation states and surface species on Pd/CeO₂ under reaction conditions, suggested reaction mechanism", *J. Catal.*, **237** (1), 17 (2006).
- [5] Chin, S. Y. Alexeev, O. S. and Amiridis, M. D., "Preferential oxidation of CO under excess H₂ conditions over Ru catalysts", *Appl. Catal. A.*, **286** (2), 157 (2005).
- [6] Han, Y. F. Kahlich, M. J. Kinne, M. and Behm, R. J., "CO removal from realistic methanol reformate via preferential oxidation – performance of an Rh/MgO

- catalyst and comparison to Ru/ γ -Al₂O₃, and Pt/ γ -Al₂O₃", *Appl. Catal. B.*, **50** (4), 209 (2004).
- [7] Chang, L. H. Sasirekha, N. and Chen, Y. W., "Au/MnO₂–TiO₂ catalyst for preferential oxidation of carbon monoxide in hydrogen stream", *Catal. Commun.* **8** (11), 1702 (2007).
- [8] Deng, W. L. Jesus, J. D. Saltsburg, H. and Flytzani-Stephanopoulos, M., "Low-content gold-ceria catalysts for the water–gas shift and preferential CO oxidation reactions", *Appl. Catal. A.*, **291** (1-2), 126 (2005).
- [9] Wang, H. Zhu, H. Q. Qin, Z. F. Wang, G. F. Liang, F.X. and Wang, J. G., "Preferential oxidation of CO in H₂ rich stream over Au/CeO₂–Co₃O₄", *Catal Commun.*, **9** (6), 1487 (2008).
- [10] Teng, Y. H. Sakurai, A. Ueda and Kobayashi, T., "Oxidative removal of CO contained in hydrogen by using metal oxide catalysts", *Int. J. Hydrogen Energy*, **24** (4), 355 (1999).
- [11] Guo, Q. and Liu, Y., "MnO_x modified Co₃O₄–CeO₂ catalysts for the preferential oxidation of CO in H₂-rich gases", *Appl. Catal. B.*, **82** (1-2), 19 (2008).
- [12] Kang, M. Song M. W. and Lee, C. H. "Catalytic carbon monoxide oxidation over CoO_x/CeO₂ composite catalysts", *Appl. Catal. A.*, **251** (1), 143 (2003).
- [13] Cheekatamarla, P. K. Epling, W. S. and Lane, A. M., "Catalytic Autothermal Reforming of Diesel Fuel for Hydrogen Generation in Fuel Cells", *J. Power Sources*, **152**, 256 (2005).
- [14] Avgouropoulos, G. Ioannides, T. and Matralis, H. "Influence of the preparation method on the performance of CuO–CeO₂ catalysts for the selective oxidation of CO", *Appl. Catal. B.*, **56** (1-2), 87 (2005).
- [15] Marba, n. G. and Fuertes. A. B., "A general and low-cost synthetic route to high-surface area metal oxides through a silica xerogel template", *App. Catal. B.*, **57** (1), 43 (2005).
- [16] karimi, A. Fatehifar, E. and Alizadeh, R. "synthesis and characterization of nanostructured CuO/CeO₂ catalyst via ultrasound assisted techniques used for selective oxidation of CO", *IJChE*, **10** (3), 50 (2013).
- [17] Sedmak, G. and Stanko, H. C., "Kinetics of selective CO oxidation in excess of H₂ over the nanostructured Cu_{0.1}Ce_{0.9}O₂–y catalyst", *J. Catal.*, **213** (2), 135 (2003).
- [18] Guimaraes, C. and Assaf, M., "Hydrogen purification for fuel cell using CuO/CeO₂–Al₂O₃ catalyst", *J. Power Sources*, **196** (2), 747 (2011).
- [19] Pouretedal, H. and Kadkhodaie, R. A., "Synthetic CeO₂ nanoparticle catalysis of methylene blue photodegradation: kinetics and mechanism", *Chin J Catal.*, **31** (11), 1328 (2010).
- [20] Zhang, J. and Ostrovski, O., "Iron ore reduction/ cementation experimental results and kinetic modeling", *Ironmak. Steelmak*, **29** (1), 15 (2002).
- [21] Zheng, X. Wang, S. Zhang, S. Wang, S. r. Huang, W. p. and Wu, S. H., "Characterization and CO oxidation behavior of CuO/CeO₂ catalysts", *React Kinet. Catal. L.*, **84** (1), 29 (2005).
- [22] Avoguropoulos, G. Ioannides, T. Matralis, H. K. Batista, and J. Hocevar, S., "CuO – CeO₂ mixed oxide catalysts for the selective oxidation of carbon monoxide in excess hydrogen", *Catal. Lett.*, **73**, 33 (2001).